A&A 409, L41–L45 (2003)
DOI: 10.1051/0004-6361:20031337

Astronomy & Astrophysics

Gas and dust in the Cloverleaf quasar at redshift 2.5

A. Weiß[1], C. Henkel[2], D. Downes[3], and F. Walter[4]

[1] IRAM, Avenida Divina Pastora 7, 18012 Granada, Spain
[2] MPIfR, Auf dem Hügel 69, 53121 Bonn, Germany
[3] IRAM, 300 rue de la Piscine, 38406 St-Martin-d'Héres, France
[4] NRAO, PO Box O Socorro, NM, 87801, USA

Received 22 August 2003 / Accepted 1 September 2003

Abstract. We observed the upper fine structure line of neutral carbon, C I($^3P_2 \rightarrow ^3P_1$) ($\nu_{\rm rest}$ = 809 GHz), the ^{12}CO(J = 3→2) line ($\nu_{\rm rest}$ = 345 GHz) and the 1.2 mm continuum emission from H1413+117 (Cloverleaf quasar, z = 2.5) using the IRAM interferometer. Together with the detection of the lower fine structure line (Barvainis et al. 1997), the Cloverleaf quasar is now only the second extragalactic system, besides M 82, where *both* carbon lines have convincingly been detected. Our analysis shows that the carbon lines are optically thin and have an excitation temperature of $T_{\rm ex} \approx 30$ K. CO is subthermally excited and the observed line luminosity ratios are consistent with $n({\rm H_2}) \approx 10^{3-4}$ cm^{-3} at $T_{\rm kin}$ = 30–50 K. Using three independent methods (C I, dust, CO) we derive a total molecular gas mass (corrected for magnification) of $M({\rm H_2}) \approx 1.2 \pm 0.3 \times 10^{10}\,M_\odot$. Our observations suggest that the molecular disk extends beyond the region seen in CO(7–6) to a zone of more moderately excited molecular gas that dominates the global emission in C I and the low J CO lines.

Key words. galaxies: formation – galaxies: starburst – galaxies: high-redshift quasars: emission lines – quasars: individual H1413+117 – cosmology: observations

1. Introduction

Detections of large amounts of dust and gas in distant quasars have opened the possibility to study molecular gas properties in the early epoch of galaxy formation and to provide fundamental constraints on galaxy evolution. To date, CO emission has been detected in more than a dozen quasar host galaxies with $z > 2$, the record holder being at $z = 6.4$ (Walter et al. 2003; Bertoldi et al. 2003). Molecular gas masses in excess of $10^{10}\,M_\odot$ have led to the hypothesis that the tremendous far–infrared (FIR) luminosities ($>10^{12}\,L_\odot$) of these objects are not only powered by active galactic nuclei (AGN) but also by major starbursts which might be forming cores of elliptical galaxies or bulges of massive spiral galaxies.

Due to its strong magnification by gravitational lensing H1413+117 is a relatively strong emitter in various molecular lines and therefore a prime target to study the physical conditions of the molecular gas at high redshift in great detail. It has been detected in the CO 3–2 (Barvainis et al. 1994; Wilner et al. 1995; Alloin et al. 1997; Barvainis et al. 1997, B97 hereafter), 4–3, 5–4 (B97) and 7–6 (Alloin et al. 1997; Yun et al. 1997) transitions, the lower fine structure line of atomic carbon, C I($^3P_1 \rightarrow ^3P_0$), (B97) and in HCN (B97, Solomon et al. 2003).

In this letter we report on the detection of the upper fine structure line of neutral carbon, C I($^3P_2 \rightarrow ^3P_1$), which adds an important piece of information: unlike CO, cool C I can be described by a 3-level system. This allows us to derive its excitation and to constrain the physical gas conditions by observations of the C I($^3P_1 \rightarrow ^3P_0$) and C I($^3P_2 \rightarrow ^3P_1$) transitions only. We compare our results from C I with estimates based on thermal dust emission and CO. We use H_0 = 75 km s^{-1} Mpc^{-1} and q_0 = 0.5.

Send offprint requests to: A. Weiß, e-mail: aweiss@iram.es

2. Observations and results

Observations were carried out with the IRAM Plateau de Bure interferometer during 2 nights in March 2003. The dual frequency setup was used to observe the ^{12}CO(J = 3→2) and C I($^3P_2 \rightarrow ^3P_1$) transitions towards H1413+117 (RA 14:15:46.23, Dec 11:29:44.0; J2000) simultaneously. The receivers were tuned in single sideband mode (SSB) at 97.191 GHz and in dual sideband mode at 224.478 GHz/227.478 GHz. We used the standard D configuration (6 antennas) which results in synthesized beams of 7.″5 × 4.″4 and 3.″5 × 1.″7 for the 3 mm and 1 mm bands respectively. At these resolutions the source is unresolved. Typical SSB system temperatures were ≈120 K and ≈300 K at 3 mm and 1 mm. Flux and passband calibration were obtained on MWC 349. The nearby sources 1413+135 and 1423+146 were used as secondary flux and phase calibrators. We estimate the flux density scale to be accurate to about 10%.

The data were processed to give data cubes with a velocity resolution of 10 km s^{-1} (3.24 MHz) at 3 mm and 40 km s^{-1}

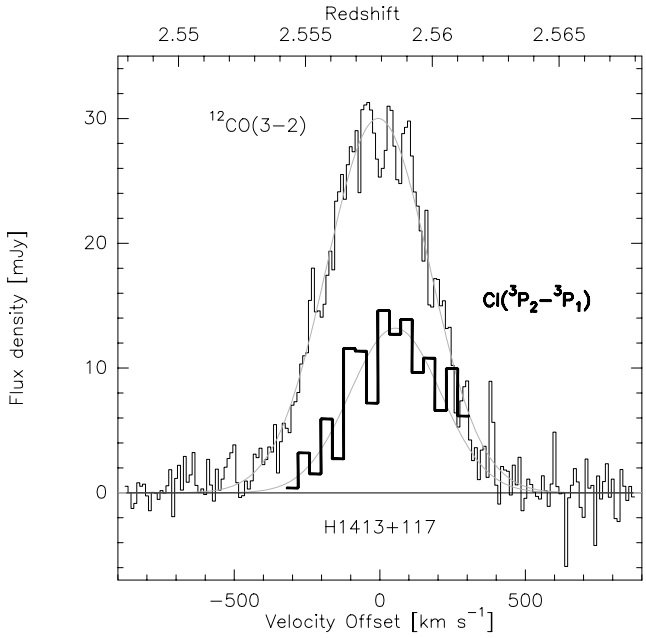

Fig. 1. Spectra of the ^{12}CO(J = 3→2) and C I(^{3}P$_2$→^{3}P$_1$) lines towards H1413+117, superposed on their Gaussian fit profiles (see Table 1 for parameters). The velocity scale is relative to the tuning frequencies of 97.191 and 227.478 GHz corresponding to z = 2.5579.

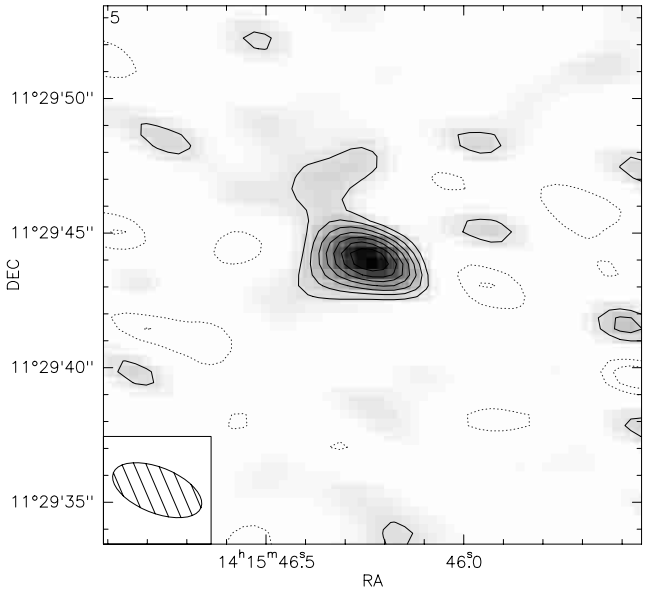

Fig. 2. Integrated C I(^{3}P$_2$→^{3}P$_1$) intensity distribution in H1413+117. Contours are plotted at −1.5, −1.0 and from 1.0 to 4.0 in steps of 0.5 Jy beam^{-1} km s^{-1}. The rms noise is 0.5 Jy beam^{-1} km s^{-1}, the peak flux density is 4.3 Jy beam^{-1} km s^{-1}. The continuum has been subtracted.

(29.7 MHz) at 1 mm. A 3 mm continuum image was generated by averaging the line emission–free channels. At 1 mm the continuum image was computed from the image sideband. From the 1 mm signal sideband data we generated a continuum free C I(^{3}P$_2$→^{3}P$_1$) spectral line cube by subtracting the 1 mm continuum image. The final results are presented in Figs. 1 and 2.

The ^{12}CO(J = 3→2) transition ($\nu_{\rm rest}$ = 345.796 GHz) is detected with high signal to noise (Fig. 1). Line parameters for the ^{12}CO(J = 3→2) transition are similar to those reported by Wilner et al. (1995) and B97. The high quality of our ^{12}CO(J = 3→2) spectrum allows us to determine the redshift of the molecular gas (as traced by CO) with high accuracy: $z = 2.55784 \pm 0.00003$.

The C I(^{3}P$_2$→^{3}P$_1$) line ($\nu_{\rm rest}$ = 809.342 GHz, Müller et al. 2001) is clearly detected with a peak flux density of $S_\nu = 13.2 \pm 2.9$ mJy (Figs. 1 and 2). Due to the limited bandwidth of 512 MHz (670 km s^{-1}) our observations lack the red line–wing. However, this does not affect the determination of the peak line intensity since the zero power level is well defined in interferometric observations. Table 1 summarizes the line parameters derived from Gaussian fits. The C I(^{3}P$_2$→^{3}P$_1$) line ($z = 2.5585 \pm 0.0001$) is displaced by ≈+60 km s^{-1} relative to ^{12}CO(J = 3→2) – opposite to the displacement of the C I(^{3}P$_1$→^{3}P$_0$) transitions found by B97 (≈–42 km s^{-1}). While the difference between the CO and C I(^{3}P$_1$→^{3}P$_0$) redshift might be attributed to low level baseline instabilities in the 30 m data and the poor signal to noise ratio, the reason for the shift in the C I(^{3}P$_2$→^{3}P$_1$) line is unclear. Gravitational amplification should not alter the center frequency for C I unless its distribution is different from CO, which we consider unlikely (see below). The apparent line shift needs to be confirmed by higher–sensitivity observations. If confirmed, this shift is most likely due to an opacity effect.

For the dust flux, we derive an upper limit for the 3 mm ($\lambda_{\rm rest}$ = 870 μm) continuum of $S_{97.2\,\rm GHz} < 1.5$ mJy (3 σ). For the 1 mm ($\lambda_{\rm rest}$ = 375 μm) continuum we find $S_{224.5\,\rm GHz} = 7.5 \pm 0.6$ mJy. We obtained an additional 250 GHz flux measurement using the MAMBO 117 channel bolometer array at the IRAM 30 m telescope with $S_{250\,\rm GHz} = 16 \pm 2$ mJy, consistent with a previous measurement (Barvainis et al. 1995). The radio–IR spectral energy distribution (SED) of H1413+117 is shown in Fig. 3.

3. Analysis

3.1. Atomic carbon

3.1.1. Opacities and excitation

Recent studies of the Milky Way and nearby galaxies showed that C I is closely associated with the CO emission independent of the environment (see e.g. Bennett et al. 1994, Ojha et al. 2001 for the MW; and Gerin & Phillips 2000, Israel & Baas 2002 for nearby galaxies). Since the critical density for the C I lines and ^{12}CO(J = 1→0) are both $n_{\rm cr} \approx 10^3$ cm^{-3} this finding suggests that the transitions arise from the same volume and share similar excitation temperatures (e.g. Ikeda et al. 2002). This allows us to estimate the opacities of the C I transitions via a LTE analysis assuming optically thick emission in ^{12}CO(J = 1→0). Since the ^{12}CO(J = 1→0) transition has not been measured in the Cloverleaf we here adopt $L'_{^{12}{\rm CO}(J=1\rightarrow0)} = 1.1\,L'_{^{12}{\rm CO}(J=3\rightarrow2)}$ (see our discussion on the CO lines). Using the values for the line luminosities (L') as listed in Table 1 and assuming as a start $T_{\rm ex} = T_{\rm dust} = 50$ K (see below) we find that both carbon lines are *optically thin* ($\tau_{10} = 0.14$, $\tau_{21} = 0.10$). For a moderate CO opacity (as suggested by B97) optical depth

Table 1. Observed line parameters.

Line	$\nu_{\rm obs}$ [GHz]	S_ν [mJy]	$\Delta V_{\rm FWHM}$ [km s^{-1}]	I [Jy km s^{-1}]	V^a [km s^{-1}]	$L'/10^{10}$ [K km s^{-1} pc^2]	Ref.
^{12}CO($J=3\rightarrow2$)	97.1928	30.0 ± 1.7	416 ± 6	13.2 ± 0.2	−5.6 ± 2.4	18.0 ± 0.3	this paper
C I(^{3}P$_2\rightarrow{}^3$P$_1$)	227.4376	13.2 ± 2.9	368 ± 25	5.2 ± 0.3	53 ± 20	1.30 ± 0.07	this paper
C I(^{3}P$_1\rightarrow{}^3$P$_0$)	138.351	7.7 ± 0.8	430 ± 46	3.6 ± 0.4	−47 ± 24	2.4 ± 0.3	B97

Quoted errors are statistical errors from Gaussian fits. Systematic calibration uncertainty is 10%.
[a] The velocity is given relative to $z = 2.5579$, the mean redshift of the CO lines determined by B97.
CO fluxes for 3–2, 4–3, 5–4, 7–6 are: 13.2, 21.1, 24.0, 47.3 [Jy km s^{-1}]; all values except for 3–2 are from B97.
CO line luminosities L' are: 18.0, 16.1, 11.7, 10.9 [10^{10} $L_\odot$].

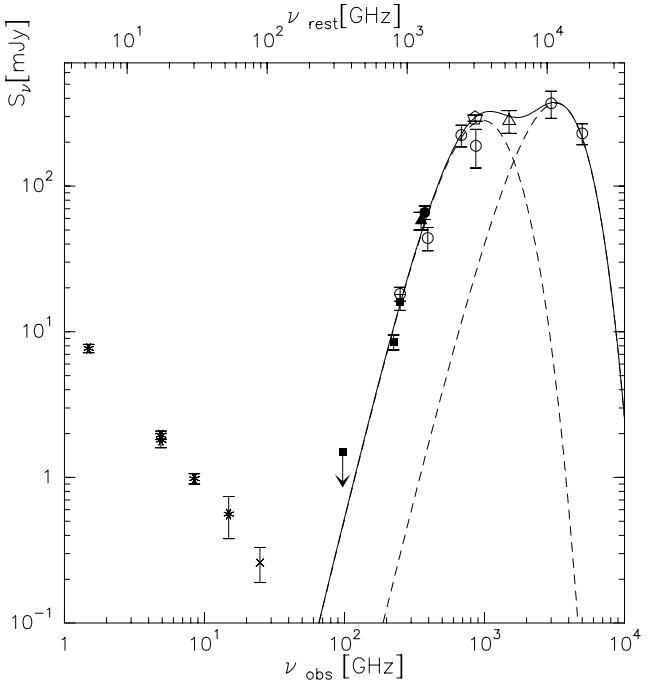

Fig. 3. Radio–IR SED of H1413+117. Displayed flux densities were taken from Barvainis & Lonsdale (1997) (20, 6, 3, 2 cm, *stars*), Solomon et al. (2003) (1.2 cm *cross*), this work (3 mm, 1.3 mm, 1.2 mm, *filled squares*), Barvainis et al. (1995) (1.2 mm, 760 μm, 438 μm, 345 μm, 100 μm, 60 μm, *circles*), Barvainis & Ivison (2002) (850 μm, *filled triangle*), Hughes et al. (1997) (800 μm, *filled circle*), Benford et al. (1999) (350 μm, *pentagon*) and Rowan-Robinson (2000) (200 μm, *triangle*). The dashed lines show the thermal dust continuum emission for a 50 and 115 K dust component. The solid line is the total emission from both components.

for the carbon lines are even lower. Low optical depths for the C I transitions are in line with findings in nearby galaxies (e.g. Israel & Baas 2002). As discussed in Stutzki et al. (1997) the integrated line intensity ratio $R_{\rm CI}$ between the C I(^{3}P$_2\rightarrow{}^3$P$_1$) and C I(^{3}P$_1\rightarrow{}^3$P$_0$) transition can be used in the optically thin limit to determine directly the C I excitation temperature via $T_{\rm ex} = 38.8\,{\rm K}/\ln[2.11/R_{\rm CI}]$. This equation is valid if the levels are thermally populated. With $R_{\rm CI} = 0.54 \pm 0.07$ (see Table 1) we find $T_{\rm ex} = 29 \pm 3$ K. For this $T_{\rm ex}$ the C I lines are still optically thin ($\tau_{10} = 0.15$, $\tau_{21} = 0.11$).

3.1.2. Neutral carbon and molecular gas mass

The relation between the integrated C I(^{3}P$_2\rightarrow{}^3$P$_1$) brightness temperature and the beam averaged C I column density in the optically thin limit for local galaxies ($z = 0$) is given by

$$N_{\rm CI} = \frac{8\pi k\nu_{21}^2}{hc^3A_{21}}\,Q(T_{\rm ex})\,\frac{1}{5}\,{\rm e}^{T_2/T_{\rm ex}}\int T_{\rm mb}\,{\rm d}v \qquad (1)$$

where $Q(T_{\rm ex}) = 1 + 3{\rm e}^{-T_1/T_{\rm ex}} + 5{\rm e}^{-T_2/T_{\rm ex}}$ is the C I partition function. $T_1 = 23.6$ K and $T_2 = 62.5$ K are the energies above the ground state. Correcting for redshift ($\int T_{\rm mb}\,{\rm d}v \rightarrow (1+z)^{-1}\int T_{\rm mb}\,{\rm d}v$) and accounting for the area of the emission region ($\Omega_{\rm s*b}\,D_{\rm A}^2$) yields the total number of carbon atoms in the source. Here $\Omega_{\rm s*b}$ denotes the solid angle of the source convolved with the telescope beam and $D_{\rm A}$ is the angular size distance to the source. Using the definition of the line luminosity (e.g. Solomon et al. 1997) we can derive the C I mass via

$$M_{\rm CI} = C\,m_{\rm CI}\,\frac{8\pi k\nu_0^2}{hc^3A_{21}}\,Q(T_{\rm ex})\,\frac{1}{5}\,{\rm e}^{T_2/T_{\rm ex}}\,L'_{\rm CI(^3P_2\rightarrow{}^3P_1)} \qquad (2)$$

where $m_{\rm CI}$ is the mass of a single carbon atom and C is the conversion between pc^2 and cm^2. Inserting numbers to Eq. (2) yields

$$M_{\rm CI} = 4.566\times10^{-3}\,Q(T_{\rm ex})\,\frac{1}{5}\,{\rm e}^{62.5/T_{\rm ex}}\,L'_{\rm CI(^3P_2\rightarrow{}^3P_1)}[M_\odot]. \qquad (3)$$

For $T_{\rm ex} = 30$ K the mass of neutral carbon thus amounts to $M_{\rm CI} = 2.6\times10^7\,m^{-1}M_\odot$ where m is the magnification by the gravitational lens.

Deriving the mass of molecular hydrogen requires an estimate of the carbon abundance relative to H_2. We here use M 82 as a template to estimate this number. Using the results from Stutzki et al. (1997), Walter et al. (2002) and Weiß et al. (2001) we obtain [C I]/[H_2] $\approx 3\times10^{-5}$. Applying this number to the carbon mass of H1413+117 results in $M(H_2) \approx 1.4\times10^{11}\,m^{-1}\,M_\odot$.

3.2. Dust emission

The mm–wave continuum measurements combined with submm, ISO and IRAS data (for references see caption of Fig. 3) are well fitted with a 2-component dust model. To account for the steep increase of the observed flux with frequency in the

observed mm regime we used $\kappa_d(\nu_r) = 10\,(\nu_r/1\,\mathrm{THz})^\beta\,\mathrm{cm^2\,g^{-1}}$ with $\beta = 2$ (Downes & Solomon 1998). For the source solid angle of the lensed dust distribution we used $\Omega_S = \pi\, m\, \theta^2/4$ with an angular size of $\theta = 0.17''$ and a magnification of $m = 11$ for both components (Venturini & Solomon 2003). Masses and dust temperatures for both components were determined by fitting those 4 free parameters to the 12 data points above the 97.2 GHz upper limit in Fig. 3. For the cold dust component we find $T_{\rm cold} \approx 50\,(\pm 2)\,\mathrm{K}$ and $M_{\rm cold} \approx 6.7\times10^8\,m^{-1}\,M_\odot\,(\pm 12\%)$. The warm component is characterized by $T_{\rm warm} \approx 115\,(\pm 10)\,\mathrm{K}$ and $M_{\rm warm} \approx 3.9\times10^6\,m^{-1}\,M_\odot\,(\pm 60\%)$. This implies $L_{\rm FIR} \approx 2.4\times10^{13}\,m^{-1}\,L_\odot$ ($L_{\rm FIR}$ as defined by Helou et al. 1985). The fit results are displayed in Fig. 3. Parameters derived for the cold gas component are in agreement with previous studies (e.g. Hughes et al. 1997; Benford et al. 1999). Using a gas to dust mass ratio of 150 (e.g. Dunne et al. 2000) the total H_2 mass in the cold component is $M(H_2) \approx 1.0\times10^{11}\,m^{-1}\,M_\odot$ in agreement with the mass determined from C I. Note that a larger angular size of the cold component leads to lower temperatures for $T_{\rm cold}$, similarly a smaller size for the warm component will yield higher $T_{\rm warm}$.

3.3. CO lines

Our ^{12}CO(J = 3→2) flux density is about 30% higher than the value reported by B97. The flux difference has important implications for the interpretation of the CO L' ratios: now the 3–2, 4–3, 5–4, 7–6 CO line luminosities (see footnote in Table 1) are decreasing with increasing J. So the data suggest CO is *subthermally excited*, at least for $J > 3$. The minimum kinetic temperature therefore can be lower than the lower limit of 60 K given in B97. We have reanalyzed the CO ratios using our 3–2 flux and taking the background radiation of $T_{\rm CMB} = 9.6\,\mathrm{K}$ into account. Due to the high 7–6 line luminosity relative to 5–4 not all CO lines can be fitted with a single gas component LVG model. If only the 3–2, 4–3 and 5–4 lines are taken into account LVG solutions can be found for $T_{\rm kin} \geq 10\,\mathrm{K}$. Since the kinetic temperature is expected to be close to the excitation temperature of neutral carbon (Israel & Baas 2002) we fixed the $T_{\rm kin}$ to 30 K. In a LVG space of [CO]/grad(V) from 1×10^{-5} to 2×10^{-4} and $\log(n_{H_2})$ 1.8 to 5.5, the allowed H_2 density ranges from $3.2 \leq \log(n_{H_2}) \leq 4.0$ with the higher limit corresponding to the lowest abundance per velocity gradient and vice versa. Independently of the abundance per velocity gradient or the density we find that for $T_{\rm kin} = 30\,\mathrm{K}$ the ^{12}CO(J = 1→0) transition will be brighter than ^{12}CO(J = 3→2) with $L'_{^{12}\mathrm{CO}(J=3\to2)}/L'_{^{12}\mathrm{CO}(J=1\to0)} \approx 0.9$, consistent with the lower limit of 0.79 determined by Tsuboi et al. (1999). Using this line ratio and $M_{H_2}/L'_{\rm CO} = 0.8\,M_\odot\,(\mathrm{K\,km\,s^{-1}\,pc^2})^{-1}$ (Downes & Solomon 1998) we get $M(H_2) \approx 1.6\times10^{11}\,m^{-1}\,M_\odot$ in agreement with the result for C I and the dust. Using $T_{\rm kin} = T_{\rm dust} = 50\,\mathrm{K}$ does not alter the results significantly. The predicted 7–6/3–2 ratio ranges between 0.05 – 0.1, much lower than the observed ratio of 0.6. A large fraction of the 7–6 line may therefore arise from much warmer regions such as the warm dust component. This is also supported by a minimum CO(7–6) excitation temperature of ≈75 K that can be derived from the observed 7–6 brightness temperature. We do not think that selective magnification would significantly alter this analysis, because detailed models of the Cloverleaf lens show that the lens magnification is insensitive to the size of the mm–line emitting region (Venturini, private communication).

4. Discussion

The mass estimates from C I, dust, and CO give remarkably similar results given that each method uses independent assumptions (carbon abundance, gas to dust mass ratio, CO conversion factor). Correcting for magnification we find $M(H_2) \approx 1.2 \pm 0.3 \times 10^{10}\,M_\odot$.

Compared to the physical conditions of the molecular gas determined in other dusty quasars ($T_{\rm kin} \approx 50$–$70\,\mathrm{K}$, $n(H_2) \approx 10^4$, see e.g. Downes et al. 1999; Carilli et al. 2002) and local ULIRGs (Downes & Solomon 1998) the values determined above for H1413+117 argue for a more diffuse and cooler gas component. Judging from the excitation temperature of C I, the excitation of the molecular gas is between conditions found in M 82's center ($T_{\rm ex,CI} = 50$ K) and the mean value over the Galactic Center ($T_{\rm ex,CI} = 22$ K) (Stutzki et al. 1997). The continuum to line ratio of $L_{\rm FIR}/L'_{\rm CO} \approx 120\,L_\odot\,(\mathrm{K\,km\,s^{-1}\,pc^2})^{-1}$ is within the range found in local ULIRGs (Solomon et al. 1997) but lower than values estimated for dusty quasars (e.g. Carilli et al. 2002; Walter et al. 2003). All this implies that large amounts of molecular gas are less affected by the heating from the AGN and/or nuclear star formation than the region emitting in CO(7–6). A possible explanation for this finding is that the molecular disk extends beyond the central region seen in CO(7–6) to a zone of more moderately excited molecular gas that dominates the global emission in C I and the low J CO lines.

Acknowledgements. We would like to thank R. Neri and R. Zylka for carrying out the observations at the PdBI and the 30 m telescope and S. Venturini for discussions on the lens model. IRAM is supported by INSU/CNRS (France), MPG (Germany) and IGN (Spain).

References

Alloin, D., Guilloteau, S., Barvainis, R., Antonucci, R., & Tacconi, L. 1997, A&A, 321, 24
Barvainis, R., Tacconi, L., Antonucci, R., Alloin, D., & Coleman, P. 1994, Nature, 371, 586
Barvainis, R., Antonucci, R., Hurt, T., Coleman, P., & Reuter, H.-P. 1995, ApJ, 451, L9
Barvainis, R., & Ivison, R. 2002, ApJ, 571, 712
Barvainis, R., & Lonsdale, C. 1997, AJ, 113, 144
Barvainis, R., Maloney, P., Antonucci, R., & Alloin, D. 1997, ApJ, 484, 695
Benford, D. J., Cox, P., Omont, A., Phillips, T. G., & McMahon, R. G. 1999, ApJ, 518, L65
Bennett, C. L., Fixsen, D. J., Hinshaw, G., et al. 1994, ApJ, 434, 587
Bertoldi, F., Cox, P., Neri, R., et al. 2003, A&A, 409, L47
Carilli, C. L., Kohno, K., Kawabe, R., et al. 2002, AJ, 123, 1838
Downes, D., & Solomon, P. M. 1998, ApJ, 507, 615
Downes, D., Neri, R., Wiklind, T., Wilner, D. J., & Shaver, P. A. 1999, ApJ, 513, L1

Dunne, L., Eales, S., Edmunds, M., et al. 2000, MNRAS, 315, 115
Gerin, M., & Phillips, T. G. 2000, ApJ, 537, 644
Helou, G., Soifer, B. T., & Rowan-Robinson, M. 1985, ApJ, 298, L7
Hughes, D. H., Dunlop, J. S., & Rawlings, S. 1997, MNRAS, 289, 766
Ikeda, M., Oka, T., Tatematsu, K., Sekimoto, Y., & Yamamoto, S. 2002, ApJS, 139, 467
Israel, F. P., & Baas, F. 2002, A&A, 383, 82
Müller, H. S. P., Thorwirth, S., Roth, D. A., & Winnewisser, G. 2001, A&A, 370, L49
Ojha, R., Stark, A. A., Hsieh, H. H., et al. 2001, ApJ, 548, 253
Rowan-Robinson, M. 2000, MNRAS, 316, 885
Solomon, P. M., Downes, D., Radford, S. J. E., & Barrett, W. J. 1997, ApJ, 478, 144
Solomon, P. M., Vanden Bout, P., & Carilli, C. L. 2003, Nature, in press
Stutzki, J., Graf, U. U., Haas, S., et al. 1997, ApJ, 477, L33
Tsuboi, M., Miyazaki, A., Imaizumi, S., & Nakai, N. 1999, PASJ, 51, 479
Venturini, S., & Solomon, P. M. 2003, ApJ, 590, 740
Walter, F., Weiß, A., & Scoville, N. Z. 2002, ApJ, 580, L21
Walter, F., Bertoldi, F., Carilli, C. L., et al. 2003, Nature, 424, 406
Weiß, A., Neininger, N., Hüttemeister, S., & Klein, U. 2001, A&A, 365, 571
Wilner, D. J., Zhao, J. H., & Ho, P. T. P. 1995, ApJ, 453, L91
Yun, M. S., Scoville, N. Z., Carrasco, J. J., & Blandford, R. D. 1997, ApJ, 479, L9